Robotics: Science and Systems 2023
Daegu, Republic of Korea, July 10-July 14, 2023

Adaptive Tracking Control of Dielectric Elastomer Soft Actuators with Viscoelastic Hysteresis Compensation

Yunhua Zhao, Li Wen
School of Mechanical Engineering and Automation, Beihang University, Beijing, China

***Abstract*—This paper proposes a new adaptive control method with viscoelastic hysteresis compensation for high-precision tracking control of dielectric elastomer actuators (DEAs). A direct inverse feedforward compensator is constructed by using a modified Prandtl-Ishlinskii model for compensating hysteresis nonlinearities. The dynamics effects of DEAs and disturbances are coped with the adaptive inverse controller using filtered-x normalized least mean square algorithm. A series of real-time tracking experiments are carried out on a DEA made of commercial acrylic elastomers. The proposed control method achieves accurate tracking of various trajectories with the relative root-mean-square tracking error ranging from 1.37% to a maximum of 4.37% over the whole operating frequency range, and outperforms previously proposed methods in terms of accuracy. The excellent tracking results demonstrate the effectiveness of the developed control method for dielectric elastomer artificial muscles based soft actuators.**

Keywords-dielectric elastomer actuators; tracking control; adaptive inverse control; hysteresis compensation; Prandtl-Ishlinskii model

I. INTRODUCTION

Dielectric elastomer actuators (DEAs) exhibit a collection of performances to be the next-generation artificial muscles, such as large deformation, fast response, high energy density, moderate bandwidth, low power consumption, and mechanical impedance comparable with human skin [1–3], making them particularly attractive for many soft robotic applications. The basic structure of a DEA consists of an elastomeric layer sandwiched between two compliant electrodes, and the essential physics of dielectric elastomer actuation are based on the deformation of a soft elastomer in response to the electric field-induced Maxwell stress when a voltage is applied through the thickness of the membrane. Some soft robots driven by DEAs have been developed for various applications such as pipeline inspection [4] and deep-sea exploration [5], but they are still far away from realistic use. In addition to the high voltage requirements and short life cycles due to various types of failures, precise control of DEAs is also a critical issue which needs to be properly addressed. However, extensive research efforts have focused on developing high-performance DEAs by improving fabrication technique and/or elastomers and electrode materials [6, 7]. High-precision tracking control of DEAs is neglected in comparison. The precise control of DEAs is challenging because they are inherently nonlinear due to the visco-hyperelasticity of large-deformation elastomer and the quadratic nonlinearity related to the electromechanical coupling. This motivates the current article to propose a control strategy, which can effectively compensate for these nonlinearities over the whole operating frequency range.

A. Related Work

The early attempts have been concentrated on feedback control, especially proportional-integral-derivative (PID) control because it could utilize the real-time output information to deal with uncertainties. For instance, Randazzo et al. [8] used classical PID controllers for regulating both position and force of a rotational joint driven by two DEAs arranged in an antagonistic configuration. Afterward, Yun and Kim [9] implemented a digital PID controller with an integrator anti-windup scheme used for reducing the performance degradation due to actuator saturation. Chuc et al. [10] implemented a pulsewidth-modulated PID feedback controller based on a high-voltage switching circuit to control the motion of a stacked DEA. Different from above standard PID regulators, a linear PID controller was cascaded with a simple square root function to limit the nonlinearity effect due to the quadratic voltage-strain relationship of DEAs [11]. Here the PID control law was developed by performing linearization of the controlled plant dynamics around a predefined equilibrium point corresponding to a constant input. However, this design method based on model linearization results in controllers having satisfactory performance only around the linearization point. To overcome this limitation, starting by establishing a dynamic model, Rizzello et al. [12] developed a robust control approach using tools from linear parameter-varying control theory and linear matrix inequality optimization. The controller, which had the form of a PID control law, could achieve output regulation with guaranteed performances in the whole operating range of the system.

The pertinent literature on feedback control of DEAs focuses almost entirely on the compensation of quadratic nonlinearity related to the DEA transduction principle, without taking into consideration inherent viscoelasticity although it is significant for dielectric elastomers especially commonly used acrylic elastomers (such as commercial 3M VHB adhesive tape). Therefore, corresponding controllers were designed mostly for tracking the trajectories at fairly low frequencies (quasi-static process) and step signals. Owing to inherent material viscoelasticity, DEAs exhibit hysteresis coupled with

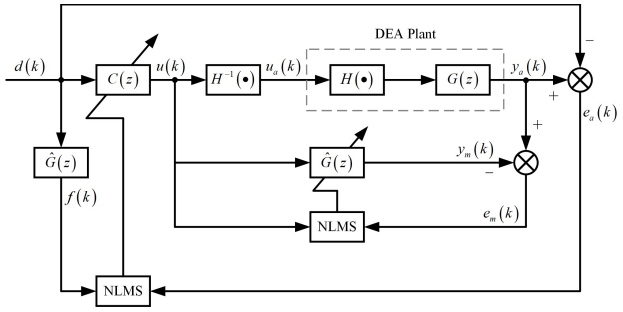

Fig. 1: Block diagram of the proposed control scheme.

creep when subjected to cyclic voltage loading, making precise control of DEAs difficult. Existing research on dealing with viscoelastic effects was concentrated on the feedforward control, which utilized known plant models to generate the control input. Using the principles of non-equilibrium thermodynamics, Gupta et al. [13] developed a dynamic model relating the displacement response to the applied voltage. A feedforward controller was then designed based on this model to track the staircase trajectory and periodic motions not exceeding 0.5 Hz. In addition to physical modeling, phenomenological modeling approach was also used to describe viscoelastic behaviors because of no need to consider the physical nature. Creep, a drift phenomenon of output displacement over time upon constant loading, can only be obviously observed in the first several cycles when subjected to cyclic voltage and becomes negligible after a few cycles [14]. The creep effect has been characterized by some well-defined models [14–16] and could be easily removed by a simple feedforward compensator [16] or a classical PI controller [17]. In contrast, viscoelastic hysteresis between input voltage and output displacement is a non-smooth nonlinearity over the whole response, and has been described by some phenomenological models [18–21]. Zou and Gu [22] then developed a two-level control architecture in the open-loop mode, consisting of a direct inverse hysteresis compensator cascaded with a feedforward creep compensator, to track sinusoidal trajectories.

However, the feedforward control cannot correct the tracking errors caused by model uncertainties and external disturbances, and the output of DEAs is easily affected by external disturbances due to inherent softness of materials. Furthermore, it should be noted that the existing control approaches could only achieve trajectory tracking within the range of fairly low frequency (not exceeding 1.5 Hz for VHB based DEAs), far below the attainable operating frequency (VHB based DEAs could still exhibit millimeter-scale displacement responses even at 11 Hz [23]); the hysteresis loops in DEAs are highly rate-dependent even showing ill-condition under the relatively high-frequency excitation [21], in which case these controllers may no longer be effective. High-precision tracking control of DEAs over the whole operating frequency range is still intractable and needs to be settled.

B. Contribution

In this work, we develop an adaptive control strategy with viscoelastic hysteresis compensation that enables a soft DEA to track trajectories accurately. First, we design a compensator based on the modified Prandtl-Ishlinskii (MPI) model to eliminate the hysteresis nonlinearity. The MPI model utilizes the play operator as the elementary operator but adopts a five-order polynomial function to replace the linear function in the classical Prandtl-Ishlinskii (P-I) model, which enables it to describe the asymmetric hysteresis behavior of DEAs. We then use an adaptive inverse controller, in series with the hysteresis compensator, to tackle the varying dynamic effect of DEAs. The controller parameters are automatically adjusted by utilizing the tracking error according to certain update strategy, to guarantee the tracking performance.

The novelty of our control approach lies first in dealing with the nonlinearity and dynamics of soft DEAs separately. Previous studies considering hysteresis nonlinearity of DEAs either just ignored the dynamic effect [17] or directly established rate-dependent and amplitude-dependent hysteresis models by redefining density function or elementary hysteresis operators [20, 22], which resulted in high model complexity. Also, as will be shown later, the feedforward control based on these models does not yield satisfactory performance especially in high-frequency trajectory tracking, while our control approach can accurately track various trajectories over the whole operating frequency range of DEAs. Secondly, the introduction of adaptive inverse control not only avoids the possible instability caused by signal feedback, but also can tackle model uncertainties and disturbances.

C. Structure

The remainder of this paper is structured as follows. In Section II, the proposed control method including an overview of control framework, the design of hysteresis compensator and adaptive controller is given. In Section III, the parameters of the inverse hysteresis model are identified and viscoelastic hysteresis compensation is implemented. In Section IV, the experimental tracking results of the developed control method on the real DEAs are presented and the tracking performance on the trajectories with different frequencies is quantitatively evaluated. The results of the developed adaptive hybrid control are also compared with those of only feedforward hysteresis compensation. Finally, a brief conclusion is given in Section V.

II. CONTROL SCHEME

A. Overview

The hysteresis loops exhibited by the DEAs are asymmetric and highly rate-dependent, and even ill-conditioned (i.e. non-positive gradient at some segments of the hysteresis curve). It has been demonstrated in previous work that the DEA can be well modeled as a Hammerstein system, the cascade of static hysteresis $H(\cdot)$ and linear dynamics $G(z)$ [21]. An adaptive hybrid control method is then proposed to achieve high-precision trajectory tracking and the block diagram represented in the discrete-time domain is depicted in Figure 1. The signals $d(k)$ and $y_a(k)$ respectively denote the desired trajectory and the actual output displacement of the DEA. The inverse

Identify applicable sponsor/s here. *(sponsors)*

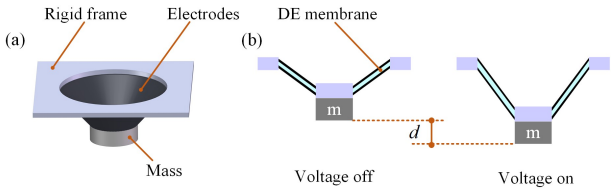

Fig. 2: (a) Schematic of the DEA; (b) Actuating principle.

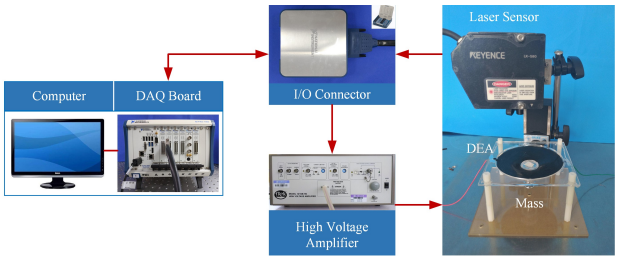

Fig. 3: Experimental setup for DEA testing and control.

hysteresis $H^{-1}(\cdot)$ is applied to compensate for the static asymmetric hysteresis based on a MPI model, while the dynamic effects are dealt with using the adaptive inverse controller $C(z)$. The controller $C(z)$ is constructed as a finite-impulse- response (FIR) filter and the corresponding weight coefficients are auto-tuning according to the filtered-x normalized least mean square (Fx-NLMS) algorithm to minimize the tracking error $e_a(k)$. $u(k)$, the output of $C(z)$, is fed to the hysteresis compensator $H^{-1}(\cdot)$, generating the control voltage.

B. Viscoelastic hysteresis compensator

The key to compensating the hysteresis nonlinearity in DEAs is the inverse of viscoelastic hysteresis. It is known that the static hysteresis loops in DEAs are asymmetric [17, 21]. The classical P-I model [24], comprising a linear input function and weighted play operators, is inappropriate for describing asymmetric hysteresis because the play operator is a hysteresis operator with symmetric and rate-independent properties. Hence the hysteresis compensator is designed with a MPI model, which is expressed as

$$V(t)=F[y](t)=g[y](t)+\int_0^R q(r)H_r[y](t)dr, \qquad (1)$$

where $g[y](t)=\sum_{i=1}^{6}\beta_i y^{6-i}(t)$, a five-order polynomial function with six coefficients $\beta_i\,(i=1,2,\cdots,6)$, is utilized to characterize the asymmetric hysteresis behavior of DEAs, and $q(r)$ is a density function. $V(t)$ and $y(t)$ represent the applied voltage and the displacement response of the DEA, respectively. For any piecewise monotone input function $y(t)\in C[0,T]$, the one-side play operator $H_r[y](t)$ with a threshold $r\geq 0$ is defined as

$$H_r[y](t)=\begin{cases} h_r(y(0),0), t=0 \\ h_r(y(t),H_r[y](t_i)), t_i<t\leq t_{i+1} \end{cases}, \qquad (2)$$

with

$$h_r(U,W)=\max(U-r,\min(U,W)), \qquad (3)$$

where $0=t_0<t_1<\cdots<t_M=T$ is a partition of $[0,T]$ such that $y(t)$ is monotonic on the subinterval $[t_i,t_{i+1}]$. As can be seen, the difference between the MPI model and the classical P-I model lies in the selection of the function $g[y](t)$. In the proposed MPI model, a generalized function is introduced to replace the linear function in the classical P-I model, but the elementary operator and density function are unchanged, making the MPI model with a relatively simple formula for asymmetric hysteresis description.

For ease of implementation, the discrete form of the MPI model is adopted and can be formulated as

$$V(t)=F_d[y](t)=g[y](t)+\mathbf{w}_H^T\mathbf{H}_r[y](t), \qquad (4)$$

where $\mathbf{H}_r=[H_{r1}, H_{r2}, \cdots, H_{rK}]^T$ is the play operator vector with thresholds $r_i=(r-1)/K$, $i=1,2,\cdots,K$, and $\mathbf{w}_H=[w_{H1}, w_{H2}, \cdots, w_{HK}]^T$ is corresponding weight vector. The parameters of the inverse hysteresis model are obtained based on the experimentally measured voltage and displacement data of the DEAs at low excitation frequency (quasi-static behavior). Corresponding to minimizing the fitting error of inverse hysteresis in the identification process, the objective function is set as the mean squared error between the experimental input voltage and predicted results, expressed as

$$G(\mathbf{X})=\frac{\sum_{j=1}^{L}(err(j))^2}{L}, \qquad (5)$$

where L is the number of data points and $err(j)$ is the identification error at the jth data point.

C. Adaptive inverse controller

After compensation of hysteresis nonlinearity, the equivalent controlled object then becomes $H^{-1}(\cdot)H(\cdot)G(z)=G(z)$. An adaptive feedforward controller $C(z)$ is utilized to cope with the dynamic effect of DEAs and residual hysteresis after preliminary compensation. Its transfer function is determined by variable parameters and those parameters can be adjusted according to certain update strategy.

Identify applicable sponsor/s here. *(sponsors)*

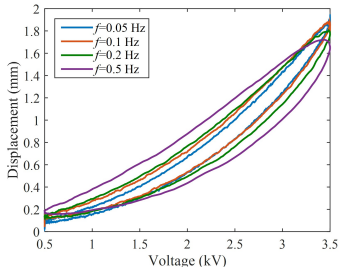

Fig. 4: Hysteresis loops of the DEA under sinusoidal excitations with different frequencies.

TABLE I. IDENTIFIED PARAMETERS OF THE MPI MODEL.

i	r_i	w_{Hi}	β_i
1	0	1.1291	0.6796
2	0.1	-0.7529	-3.9245
3	0.2	0.0414	7.0000
4	0.3	-0.0018	-5.8130
5	0.4	-0.0113	2.6384
6	0.5	0.0025	-0.0219
7	0.6	-0.0238	
8	0.7	-0.0127	
9	0.8	-0.0720	
10	0.9	-0.0541	

The FIR filter, a delayed adaptive filter, is used as the adaptive controller owing to its simplicity and ease of implementation. It is pointed out that the path from the output of the adaptive controller to the error signal, known as the secondary path, causes phase shifts or delays in signal transmission. To compensate for the effects of the secondary path, the filtered-x adaptive filter is employed where the impulse response of the secondary path is estimated and taken into consideration. The dynamics estimation of the DEA system $\hat{G}(z)$ and the adaptive inverse controller $C(z)$ are both constructed as FIR filters:

$$\hat{G}(z)=\sum_{i=0}^{N-1} v_i(k) z^{-i},\ C(z)=\sum_{j=0}^{N-1} w_j(k) z^{-j}, \tag{6}$$

where N refers to the order of both filters, and $v_i(k)$ and $w_j(k)$ are their respective coefficients (the ith weight at kth time and the jth weight at kth time). The weight coefficients $w_j(k)$ are updated by minimizing the expectation value of the squared tracking error $e_a^2(k)$, that is

$$\min\left\{E\left[e_a^2(k)\right]\right\}=\min\left\{E\left[y_a(k)-d(k)\right]^2\right\}. \tag{7}$$

Instead of standard least mean square (LMS) algorithm, the normalized LMS (NLMS) algorithm is employed to improve

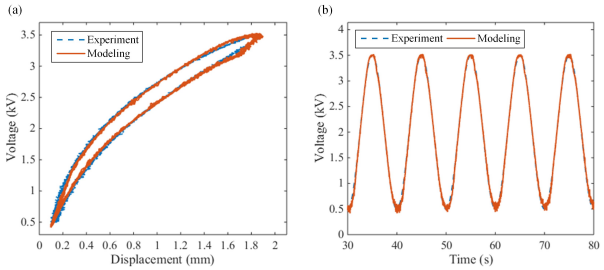

Fig. 5: Identification results. (a) Voltage versus displacement; (b) Time-series voltage.

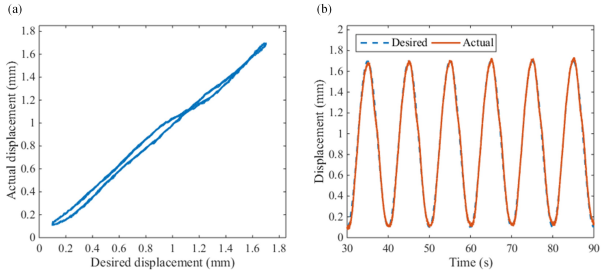

Fig. 6: Compensation for the static hysteresis. (a) Actual displacement versus desired displacement; (b) Time history of the displacement at a frequency of 0.1 Hz.

the convergence speed of adaptive filters. The filter coefficients are thus updated according to the following equation:

$$\mathbf{w}(k+1)=\mathbf{w}(k)+2\mu_c e_a(k)\frac{\mathbf{f}(k)}{\left\|\mathbf{f}(k)+p\right\|^2}, \tag{8}$$

where $\mathbf{w}(k)=\left[w_0(k), w_1(k), \cdots, w_{N-1}(k)\right]^T$ is the weight coefficient vector and p is a minor positive constant that prevents the coefficients from being infinity. The step size μ_c is determined experimentally, and the order of the FIR filter N is experimentally chosen based on the trade-off between approximation error and filter complexity. $\mathbf{f}(k)=[f(k), f(k-1), \cdots, f(k-N+1)]^T$, and $f(k)$, generated by filtering the signal $d(k)$ with $\hat{G}(z)$, satisfies

$$f(k)=\sum_{i=0}^{N-1} v_i d(k-i). \tag{9}$$

Similarly, the weight coefficients of the filter $\hat{G}(z)$ are updated according to

$$\mathbf{v}(k+1)=\mathbf{v}(k)+2\mu_m e_m(k)\frac{\mathbf{u}(k)}{\left\|\mathbf{u}(k)+p\right\|^2}, \tag{10}$$

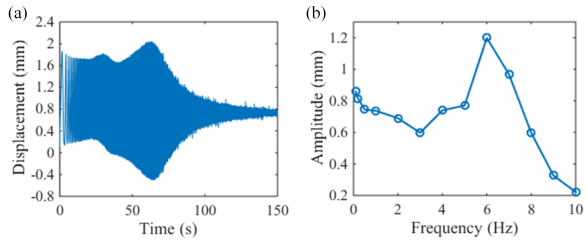

Fig. 7: (a) The DEA's displacement response under linear sweep excitation from 0.1 to 15 Hz. (b) Variation of the DEA's displacement amplitude with frequency.

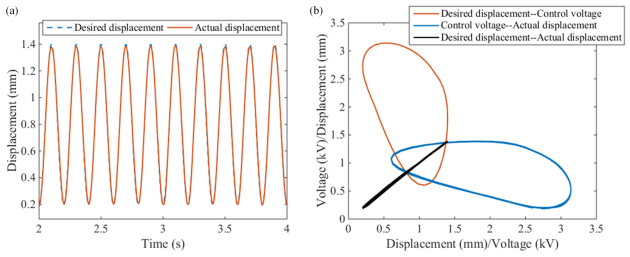

Fig. 8: (a) Tracking results for a 5 Hz sinusoidal waveform. (b) Three types of output-input relationships for the proposed controller, the direct plant and the overall closed-loop system.

where $\mathbf{v}(k)=\left[v_0(k),v_1(k),\cdots,v_{N-1}(k)\right]^T$ is the coefficients vector. Considering the model uncertainty, the estimation of the secondary path $\hat{G}(z)$ is identified online. The robustness of the NLMS algorithm to the external and internal disturbances has been proven in the literature [25, 26].

III. HYSTERESIS IDENTIFICATION AND COMPENSATION

The DEA considered in this work is based on the truncated cone-shaped geometry as shown in Figure 2a. A loading mass is connected to the moving part of the dielectric film as the end effector of the actuator. In response to a voltage applied to the electrodes, the dielectric film is squeezed in the thickness direction as a result of Maxwell stress, resulting in biaxial expansion, and the subsequent motion is illustrated in Figure 2b. The schematic diagram of the experimental setup for DEA testing and control is shown in Figure 3.

Figure 4 presents the experimental hysteresis loops in steady state at different excitation frequencies, clearly demonstrating the rate-dependence of viscoelastic hysteresis in DEAs. It is also noticed that there is pretty substantial overlap between the hysteresis loops at 0.05 Hz and 0.1 Hz. Hence an input voltage at 0.1 Hz (considered as quasi-static) was adopted to identify the parameters of the MPI model. The discretization level K was selected as 10. A matlab function *lsqnonlin* was employed to estimate the weight vector $\mathbf{w}_H$ and coefficients $\beta_i\,(i=1,2,\cdots,6)$, and the identified parameters are listed in Table I when the input and output are in normalized cases. The root-mean-square value of identification error is 0.05 kV.

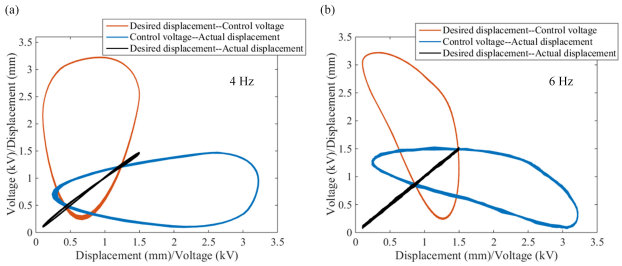

Fig. 9: Three types of output-input relationships at different frequencies.

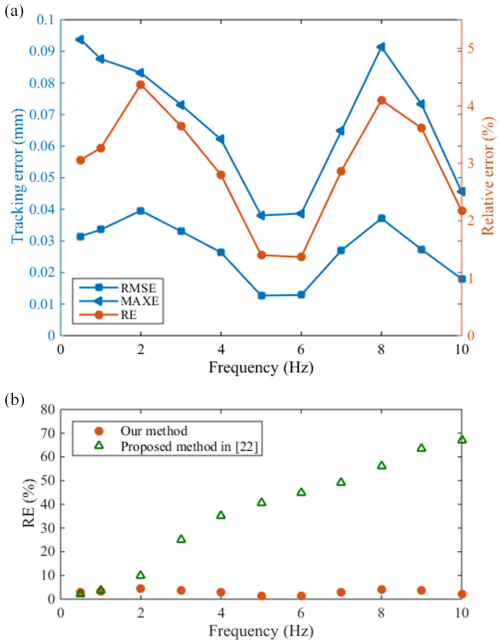

Fig. 10: (a) Tracking errors for sinusoidal waveforms of different frequencies using the adaptive control method. (b) Comparison of tracking accuracy between our adaptive control method and the control method used in [22].

Furthermore, the experimentally measured inverse hysteresis was compared with the simulated results as depicted in Figure 5. It can be seen that they are in good agreement, suggesting that the MPI model could well describe the static inverse hysteresis.

Based on the presented MPI model, the compensation for hysteresis nonlinearity of DEAs was performed. The reference trajectory was set as a sinusoidal waveform of 0.1 Hz with the amplitude of 0.8 mm and the bias of 0.9 mm, and the corresponding experimental results are shown in Figure 6. As shown in the figure, the relation between reference signal and actual displacement was approximately linear and that the desired waveform was well replicated. It should be noted that the DEAs show obviously dynamic effect, whereas the MPI model is frequency-independent, meaning that a dynamics compensator is further needed for the precise control of DEAs.

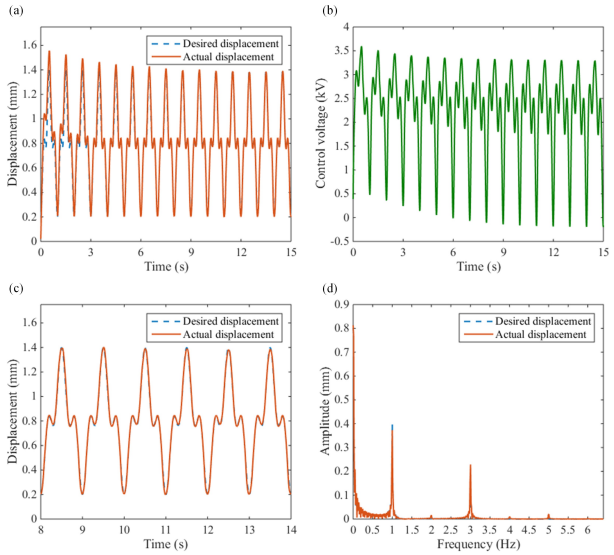

Fig. 11: Tracking results for a multi-frequency waveform using our proposed control approach: (a) Actuator displacement; (b) Control voltage. Comparison between desired displacement and actual displacement at steady state in (c) time domain and (d) frequency domain.

IV. TRAJECTORY TRACKING RESULTS

Before trajectory tracking experiments, the DEA's response bandwidth was determined. The DEA's displacement response to a linear sweep (0.1 Hz/s) input with a frequency range of 0.1-15 Hz was measured. As can be seen from Figure 7a, the displacement amplitude after 100s (corresponding to the frequency range above 10 Hz) is significantly smaller than the quasi-static amplitude. Moreover, the steady-state displacement amplitudes at frequencies from 0.1 to 10 Hz are shown in Figure 7b. It can be seen that the response amplitude reaches a maximum of 1.20 mm at 6 Hz and then decreases monotonically to 0.22 mm at 10 Hz, which is approximately 25% of the value at 0.1 Hz (i.e., 6 dB attenuation compared to the quasi-static amplitude). Hence the operating frequency range of the DEA made of commercial VHB elastomers is within 10 Hz.

The proposed adaptive control was applied to the DEA and the results of tracking a 5 Hz sinusoidal wave with the amplitude of 0.6 mm and the bias of 0.8 mm are presented in Figure 8a. As shown in the figure, the designed controller accurately tracks the reference trajectory. Further, three types of output-input relationships for the proposed controller, the direct plant and the overall closed-loop system (i.e., control voltage versus desired displacement, actual displacement versus control voltage and actual displacement versus desired displacement) are summarized in Figure 8b. It can be seen that the hysteresis loop of the DEA is significantly different from those shown in Figure 4 and exhibits noticeable ill-condition that the output displacement does not peak at the maximum applied voltage but increases continuously or remains constant somewhere. Yet still the relation between desired displacement and actual displacement is approximately linear, and the same is true for 4 Hz and 6 Hz tests (see Figure 9 where hysteresis

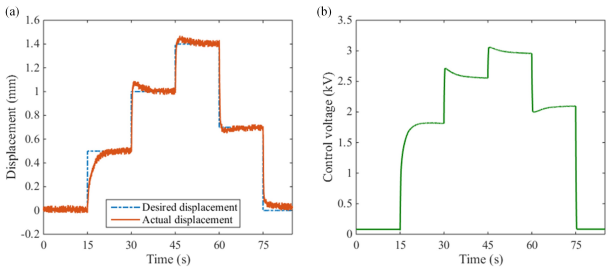

Fig. 12: (a) Tracking results for a stair-like trajectory. (b) Control voltage computed by the developed controller.

profiles are rather different), meaning that the controller is able to compensate for nonlinearities and dynamics.

To quantitatively evaluate the tracking performance, we define the root-mean-square error (RMSE), maximum error (MAXE) and relative error (RE) with respect to root-mean-square of the end effector as our performance metric:

$$RMSE = \sqrt{\frac{\sum_{k=1}^{N}\left(e_a(k)\right)^2}{N}}$$
$$MAXE = \max_k \left|e_a(k)\right| \quad . \qquad (11)$$
$$RE = \frac{\sqrt{\sum_{k=1}^{N}\left(e_a(k)\right)^2}}{\sqrt{\sum_{k=1}^{N}\left(d(k)\right)^2}} \times 100\%$$

The tracking errors for sinusoidal waveforms of different frequencies from 0.5 to 10 Hz are shown in Figure 10a. The maximum values of absolute tracking errors RMSE and MAXE are 0.040 mm and 0.094 mm respectively, and the RE value ranges from a minimum of 1.37% at 6 Hz to a maximum of 4.37% at 2 Hz, cogently suggesting that the proposed control strategy enables satisfactory trajectory tracking even though for soft DEAs with high dynamics.

In addition, our control method is compared with existing control methods for DEAs in terms of tracking accuracy. To the best of our knowledge, the control method developed in [22] is one of the few methods that take into account viscoelastic hysteresis nonlinearity of DEAs, and has the best tracking performance among them. The feedforward control approach used in [22] involves two cascaded compensators: a creep compensator and a direct inverse hysteresis compensator based on a modified rate-dependent P-I model by constructing rate-dependent play operators. The tracking errors for sinusoidal trajectories of different frequencies obtained by applying this control method are shown in Figure 10b. As can be seen from the figure, with using the feedforward control in [22], the tracking error is small over trajectories below 2 Hz, but becomes large as the trajectory frequency increases further, from 9.80% at 2 Hz to 66.81% at 10 Hz, which indicates that

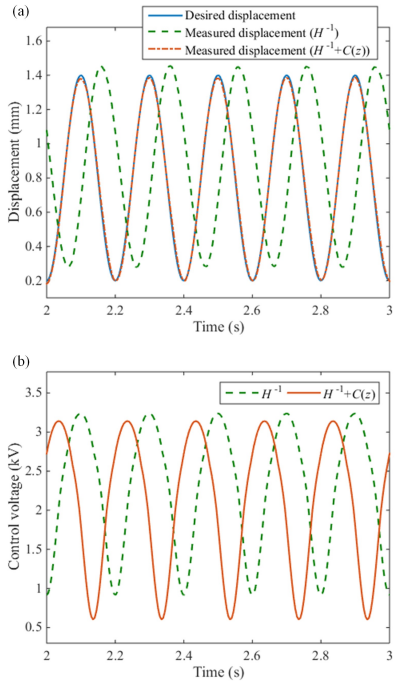

Fig. 13: Comparison of tracking results obtained by different methods: (a) Actuator displacement; (b) Control voltage.

corresponding model cannot accurately capture the dynamic behavior of DEAs. In comparison, our adaptive control method achieves high tracking accuracy (the tracking error is at a low level) over the whole operating frequency range.

When the reference trajectory is a superposition of two sinusoidal waveforms with different frequencies (1 Hz and 3 Hz), biases (0.6 mm and 0.2 mm) and amplitudes (0.4 mm and 0.2 mm), the tracking results are shown in Figure 11. It can be seen from Figure 11a that the DEA's output displacement gradually approaches the desired displacement over time, although the convergence speed is relatively slow due to fairly conservative values of the step sizes ($\mu_c = \mu_m = 0.004$). Also, as shown in Figure 11c and 11d, the actual displacement at steady state is very consistent with the desired displacement, demonstrating the excellent steady-state performance of our control approach. Moreover, the experiment of tracking a stair-like trajectory with a maximum stroke of 1.4 mm was also conducted, and the tracking results and corresponding control voltage are presented in Figure 12. As shown in the figure, the reference trajectory can be satisfactorily tracked without noticeable steady-state error. The above tracking experiments verify the feasibility of our control method for soft DEAs.

Finally, the tracking results of the developed adaptive hybrid control and only using feedforward hysteresis compensation are compared, in order to elucidate the role of the adaptive inverse controller. As can be seen from Figure 13a, when relying only on hysteresis compensator $H^{-1}(\cdot)$, the tracking performance is terrible (there is a significant difference between reference displacement and actual displacement, especially in phase). In contrast, the adaptive hybrid control achieves high tracking accuracy with a relative error of 1.40% because the generated control voltage is ahead of the desired displacement in phase (see Figure 13b). This comparison shows that the introduced adaptive inverse controller $C(z)$ is able to cope with the system dynamics.

V. Conclusion

In summary, we successfully develop an adaptive control strategy for soft DEAs. The excellent tracking performance is achieved by combining adaptive inverse control and viscoelastic hysteresis compensation. A direct inverse feedforward hysteresis compensator is designed based on a MPI model, and an adaptive inverse controller is used in series to deal with the dynamics of DEAs with coefficients being automatically updated by employing the NLMS algorithm. It is shown that our controller is able to compensate quickly and effectively for hysteresis nonlinearities and varying dynamics of soft DEAs, enabling accurate tracking of various motions over the whole operating frequency range. Additionally, our control approach outperforms the feedforward compensation approach developed in previously published papers in terms of tracking accuracy. Further work will focus on combining our control method with self-sensing algorithm to achieve sensorless tracking control for DEAs based soft robots.

Acknowledgment

We thank the Area Chairs and the anonymous reviewers for their comments and suggestions. This work was supported by the National Natural Science Foundation of China (Grant No. 92048302).

References

[1] R. Pelrine, R. Kornbluh, Q. Pei, and J. Joseph. High-Speed Electrically Actuated Elastomers with Strain Greater Than 100%. Science, 287(5454): 836–839, 2000.

[2] H. Zhao, A. M. Hussain, M. Duduta, D. M. Vogt, R. J. Wood, and D. R. Clarke. Compact Dielectric Elastomer Linear Actuators. Advanced Functional Materials, 28(42): 1804328, 2018.

[3] M. Duduta, E. Hajiesmaili, H. Zhao, R. J. Wood, and D. R. Clarke. Realizing the Potential of Dielectric Elastomer Artificial Muscles. Proceedings of the National Academy of Sciences, 116(7): 2476–2481, 2019.

[4] C. Tang et al. A Pipeline Inspection Robot for Navigating Tubular Environments in the Sub-Centimeter Scale. Science Robotics, 7(66): eabm8597, 2022.

[5] G. Li et al. Self-powered Soft Robot in the Mariana Trench. Nature, 591(7848): 66–71, 2021.

[6] Z. Peng, Y. Shi, N. Chen, Y. Li, and Q. Pei. Stable and High-Strain Dielectric Elastomer Actuators Based on a Carbon Nanotube-Polymer Bilayer Electrode. Advanced Functional Materials, 31(9): 2008321, 2021.

[7] Y. Shi et al. A Processable, High-Performance Dielectric Elastomer and Multilayering Process. Science, 377(6602): 228–232, 2022.

[8] M. Randazzo, M. Fumagalli, G. Metta, and G. Sandini. Closed Loop Control of a Rotational Joint Driven by Two Antagonistic Dielectric Elastomer Actuators. In Proceedings of SPIE Electroactive Polymer Actuators and Devices, pages 76422D, 2010.

[9] K. Yun and W. Kim. Microscale Position Control of An Electroactive Polymer Using An Anti-Windup Scheme. Smart Materials and Structures, 15(4): 924–930, 2006.

[10] N. H. Chuc et al. Fabrication and Control of Rectilinear Artificial Muscle Actuator. IEEE/ASME Transactions on Mechatronics, 16(1): 167–176, 2011.

[11] G. Rizzello, D. Naso, A. York, and S. Seelecke. Modeling, Identification, and Control of a Dielectric Electro-Active Polymer Positioning System. IEEE Transactions on Control Systems Technology, 23(2): 632–643, 2015.

[12] G. Rizzello, D. Naso, B. Turchiano, and S. Seelecke. Robust Position Control of Dielectric Elastomer Actuators Based on LMI Optimization. IEEE Transactions on Control Systems Technology, 24(6): 1909–1921, 2016.

[13] U. Gupta, Y. Wang, H. Ren, and J. Zhu. Dynamic Modeling and Feedforward Control of Jaw Movements Driven by Viscoelastic Artificial Muscles. IEEE/ASME Transactions on Mechatronics, 24(1): 25–35, 2019.

[14] G. Gu, U. Gupta, J. Zhu, L. Zhu, and X. Zhu. Modeling of Viscoelastic Electromechanical Behavior in a Soft Dielectric Elastomer Actuator. IEEE Transactions on Robotics, 33(5): 1263–1271, 2017.

[15] M. Wissler and E. Mazza. Mechanical Behavior of an Acrylic Elastomer Used in Dielectric Elastomer Actuators. Sensors and Actuators A: Physical, 134(2): 494–504, 2007.

[16] J. Zou, G. Gu, and L. Zhu. Open-Loop Control of Creep and Vibration in Dielectric Elastomer Actuators with Phenomenological Models. IEEE/ASME Transactions on Mechatronics, 22(1): 51–58, 2017.

[17] J. Zou and G. Gu. High-Precision Tracking Control of a Soft Dielectric Elastomer Actuator with Inverse Viscoelastic Hysteresis Compensation. IEEE/ASME Transactions on Mechatronics, 24(1): 36–44, 2019.

[18] Y. Zhang, K. Wang, and R. W. Jones. Characterisation, Modelling and Hysteresis Compensation in a Tubular Dielectric Elastomer Actuator. In IEEE/ASME International Conference on Advanced Intelligent Mechatronics, pages 884–889, 2010.

[19] P. Tian, R. W. Jones, and F. Yu. Elliptical Modelling of Hysteresis Operating Characteristics in a Dielectric Elastomer Tubular Actuator. Smart Materials and Structures, 25(7): 075038, 2016.

[20] J. Zou and G. Gu. Modeling the Viscoelastic Hysteresis of Dielectric Elastomer Actuators with a Modified Rate-Dependent Prandtl–Ishlinskii Model. Polymers, 10(5): 525, 2018.

[21] Y. Zhao, G. Meng, and W.-M. Zhang. Characterization and Modeling of Viscoelastic Hysteresis in a Dielectric Elastomer Actuator. Smart Materials and Structures, 29: 055019, 2020.

[22] J. Zou and G. Gu. Feedforward Control of the Rate-Dependent Viscoelastic Hysteresis Nonlinearity in Dielectric Elastomer Actuators. IEEE Robotics and Automation Letters, 4(3): 2340–2347, 2019.

[23] Y. Zhao, Q. Guo, S. Wu, G. Meng, and W. Zhang. Design and Experimental Validation of an Annular Dielectric Elastomer Actuator for Active Vibration Isolation. Mechanical Systems and Signal Processing, 134: 106367, 2019.

[24] M. Brokate and J. Sprekels. Hysteresis and Phase Transitions. New York: Springer, 1996.

[25] P. Bolzern, P. Colaneri, and G. De Nicolao. Robustness and Performance in Adaptive Filtering. In Robustness in Identification and Control. London: Springer, 1999, pages 174–189.

[26] B. Hassibi. On the Robustness of LMS Filters. In Least–Mean–Square Adaptive Filters. 2003, pages 105–144.
https://doi.org/10.1002/0471461288.ch4